An analytical model of the dual-injection-locked opto-electronic oscillator (DIL-OEO)

C. R. Menyuk,* *E. C. Levy*,† *O. Okusaga*,*,‡ *M. Horowitz*,† *G. M. Carter*,* *and W. Zhou*‡
*Computer Science and Electrical Engineering Department
University of Maryland, Baltimore, MD 21250, USA,
Email: menyuk@umbc.edu
†Department of Electrical Engineering
Technion—Israel Institute of Technology, Haifa, ISRAEL
‡U.S. Army Research Laboratory, 2800 Powder Mill Road, Adelphi, MD, USA

***Abstract*— We derive the equations that govern the phase noise at steady state in two coupled oscillators with delay. This simple model is then applied to the dual-injection-locked opto-electronic oscillator (DIL-OEO). This model is an extension of the Yao-Maleki model from one OEO loop to two, and it is complementary to other work on full simulations and experiments that we have carried out. We use this model to understand the key features of our current experiments and to point to a new regime in which the spurs can potentially be greatly reduced without greatly increasing the phase noise.**

I. Introduction

Low-phase-noise microwave oscillators have numerous applications in transmitting and receiving communications signals, in setting clock references, and in RF photonics applications like RF radar [1]. A promising and relatively new type of oscillator that produces signals in the neighborhood of 10 GHz is the opto-electronic oscillator (OEO) that was invented by Yao and Maleki [2], [3]. This oscillator uses a long length of optical fiber as a delay line. The microwave signal is imposed on an optical carrier at the beginning of the fiber and is detected at the end with a photo-detector. The optics plays the strictly passive role of transporting the RF signal over that long length. Below 1 kHz from the carrier, the OEO produces lower phase noise than the best dielectric resonant oscillators [4].

A difficulty with this configuration is that the long cavity length implies that many cavity modes can exist in an OEO. In an OEO with a 4 km fiber loop (20 μs delay), the modes are spaced 50 kHz apart. This difference is too small for the unwanted modes to be eliminated by RF filters. Instead a coupled cavity approach must be used. A number of configurations have been proposed [5]–[7].

Here, we will focus on the configuration shown in Fig. 1 that was proposed by Zhou and Blasche [6], in which two OEO loops are weakly coupled. One loop is long, and the other is short. We refer to the long OEO loop as the master loop and the short OEO loop as the slave loop. It was originally thought that power should only be injected from the master loop into the slave loop, but subsequent work made clear that back injection from the slave loop into the master loop is necessary [8]. Here, we explain this observation.

In other work, we have presented or will present a detailed simulation model and its validation by comparison to experiments [8]–[14]. In this work, we present a simple model for the phase noise that will serve as a guide to full simulations and experiments, as well as providing physical insight.

This work was supported by the Defense Advanced Research Projects Agency as part of the SILO project.

II. Review of the Yao-Maleki Model

In their original work, Yao and Maleki [3] presented a simple model of a single-loop OEO that allowed them to calculate the phase noise when the OEO operates in steady state. Subsequent work by ourselves, in which we compared their results to both full simulations and to experiments show that their results produce results that are within 3 dB of the full model [8]–[14].

In this work, we extend the work of Yao and Maleki to two coupled oscillators, both of which have delay. In this section, we will review the Yao-Maleki model and introduce the notation that will be used throughout the remainder of this paper.

We begin by defining $A(t)$, the complex carrier of the voltage at the output of the photo-detector, by writing $V(t) = A(t)\exp(2\pi j\nu_0 t)$ + complex conjugate, where $V(t)$ is the real voltage signal and ν_0 is the carrier frequency, which is typically near 10 GHz. Following the signal through one round trip of the OEO that is shown in Fig. 1, we find that $A(t)$ must satisfy the delay-difference equation

$$A(t) = GM\left[|A(t)|^2\right]A(t-\tau) + S(t), \tag{1}$$

where t is time, τ is the round-trip delay, G is the small signal gain, which we may assume is constant over the operating bandwidth of the OEO, and $S(t)$ is the noise input from which the oscillator power grows. The quantity $|A(t)|^2$ is proportional to the electrical power.

In their original work, Yao and Maleki assumed that the saturation was due to a $LiNbO_3$ modulator and has the form,

$$M(P) = 2\left(\frac{P}{P_{\rm sat}}\right)^{1/2} J_1\left[\left(\frac{P_{\rm sat}}{P}\right)^{1/2}\right], \tag{2}$$

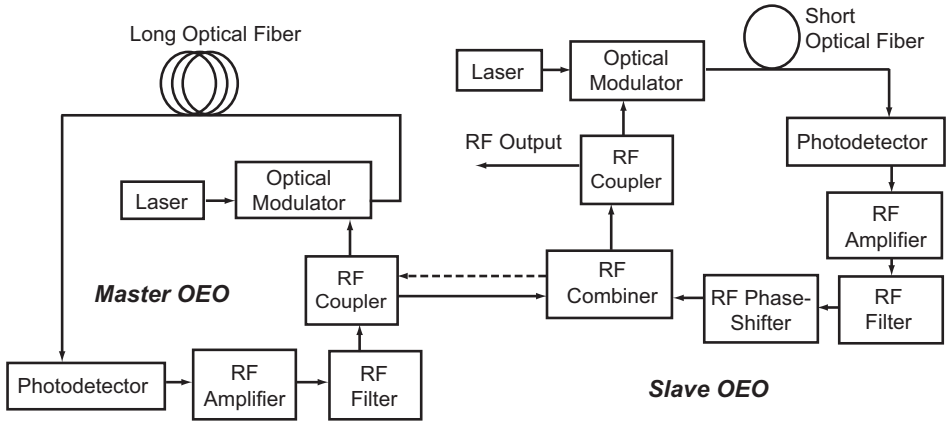

Fig. 1. Block diagram of the DIL-OEO. The back injection from the slave loop to the master loop is shown with a dashed line.

where $J_1(x)$ denotes the first Bessel function and $P_{\rm sat}$ is the saturation power. In our experimental work, the saturation is due to the RF amplifiers and has the form,

$$M(P) = \frac{1}{1 + P/P_{\rm sat}}. \tag{3}$$

This difference has no effect on the steady-state model that is presented in this paper. When the OEO operates at steady state, the quantity GM is determined by the Barkhausen condition [15] and may be treated as a constant. Once that is done, Eq. (1) becomes linear, and transforming into the Fourier domain, using the transform relations

$$\begin{aligned} \tilde{X}(\omega) &= \int_{-\infty}^{\infty} X(t) \exp(-j\omega t)\, dt, \\ X(t) &= \frac{1}{2\pi} \int_{-\infty}^{\infty} \tilde{X}(\omega) \exp(j\omega t)\, d\omega, \end{aligned} \tag{4}$$

where we use tildes to indicate the Fourier transform, we find that Eq. (1) becomes

$$\tilde{A}(\omega) = (1 - \Delta)\tilde{A}(\omega) \exp(-j\omega\tau) + \tilde{S}(\omega), \tag{5}$$

where $\Delta = 1 - GM$ will be a positive quantity that is close to zero.

From, Eq. (5), we obtain immediately

$$\tilde{A}(\omega) = \frac{\tilde{S}(\omega)}{1 - (1 - \Delta)\exp(-j\omega\tau)}. \tag{6}$$

Squaring this equation and taking an ensemble average over the noise, we find

$$P(\omega) = \frac{N(\omega)}{|1 - (1 - \Delta)\exp(-j\omega\tau)|^2}, \tag{7}$$

where $P(\omega) = \langle |A(\omega)|^2 \rangle$ and $N(\omega) = \langle |S(\omega)|^2 \rangle$ indicate respectively ensemble averages of the oscillator's power spectrum and the power spectrum of the noise that drives the oscillator. This driving noise power should not be confused with the oscillator's phase noise, which is determined by $P(\omega)$. When $j\omega\tau \ll 1$, Eq. (7) reduces to the standard Lorentzian form

$$P(\omega) = \frac{N(\omega)}{\Delta^2 + \omega^2\tau^2}. \tag{8}$$

We may determine Δ from the signal-to-white-noise ratio, assuming that the oscillator's average power W is dominated by the white noise inputs. In that case, we have $\Delta = N_{\rm w}/4\tau W$, where $N_{\rm w}$ is the one-sided power spectral density of the white noise. Flicker noise inputs may also contribute to Δ, depending on the details of how W is measured, but from dimensional arguments, we anticipate that $\Delta \sim \tau W$ in any case, and phase noise is insensitive to the actual value of Δ for the system parameters and frequency range of interest. In our experimental setting, typical values at the photo-detector output are $N_{\rm w} = -170$ dBm/Hz, $W = -23$ dBm, and $\tau = 20$ μs, from which we find $\Delta = -106$ dB.

III. Model for the DIL-OEO

Moving now to the configuration shown in Fig. 1, we obtain the coupled equations,

$$\begin{aligned} A_1(t) &= G_1 M_1 A_1(t - \tau_1) + \Gamma_{12} A_2(t) + S_1(t), \\ A_2(t) &= G_2 M_2 A_2(t - \tau_2) + \Gamma_{21} A_1(t) + S_2(t), \end{aligned} \tag{9}$$

where we use the subscripts 1 and 2 to refer to the master and slave loops, respectively, Γ_{12} indicates the coupling of the slave to the master, and Γ_{21} indicates the coupling of the master to the slave.

Proceeding by analogy with the Yao-Maleki model, we move to the Fourier domain, which yields

$$\begin{aligned} \tilde{A}_1(\omega) &= (1 - \Delta_1)\tilde{A}_1(\omega)\exp(-j\omega\tau_1) + \Gamma_{12}\tilde{A}_2(\omega) \\ &\quad + \tilde{S}_1(\omega), \\ \tilde{A}_2(\omega) &= (1 - \Delta_1)\tilde{A}_2(\omega)\exp(-j\omega\tau_2) + \Gamma_{21}\tilde{A}_1(\omega) \\ &\quad + \tilde{S}_2(\omega), \end{aligned} \tag{10}$$

from which we obtain

$$\begin{aligned} \tilde{A}_1(\omega) &= \frac{1}{D(\omega)}\{[1 - (1 - \Delta_2)\exp(-j\omega\tau_2)]\tilde{S}_1(\omega) \\ &\quad + \Gamma_{12}\tilde{S}_2(\omega)\}, \\ \tilde{A}_2(\omega) &= \frac{1}{D(\omega)}\{[1 - (1 - \Delta_1)\exp(-j\omega\tau_1)]\tilde{S}_2(\omega) \\ &\quad + \Gamma_{21}\tilde{S}_1(\omega)\}, \end{aligned} \tag{11}$$

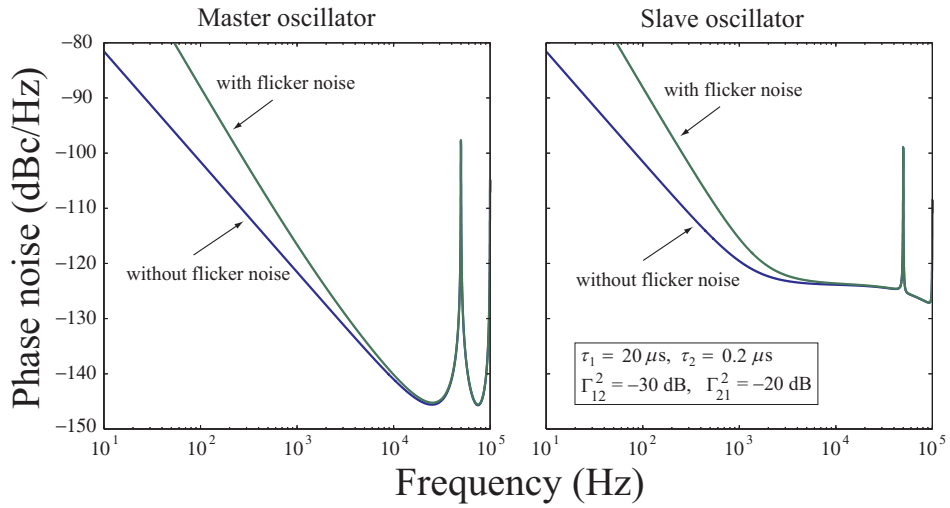

Fig. 2. Bode plots of the phase noise $\mathcal{L}(f)$ vs. frequency for both the master and slave loops. The parameters correspond to our current experiments.

where

$$D(\omega) = [1-(1-\Delta_1)\exp(-j\omega\tau_1)][1-(1-\Delta_2)\exp(-j\omega_2\tau_2)] - \Gamma_{12}\Gamma_{21}. \quad (12)$$

Finally, we square and take the ensemble average to obtain

$$\begin{aligned} P_1(\omega) &= \frac{1}{|D_1(\omega)|^2}[|1-(1-\Delta_2)\exp(-j\omega\tau_2)|^2 \\ &\quad N_1(\omega) + \Gamma_{12}^2 N_2(\omega)], \\ P_2(\omega) &= \frac{1}{|D_2(\omega)|^2}[|1-(1-\Delta_1)\exp(-j\omega\tau_1)|^2 \\ &\quad N_2(\omega) + \Gamma_{21}^2 N_1(\omega)], \end{aligned} \quad (13)$$

where we assume that the input noise power in the two loops is uncorrelated.

Equation (13) is our basic equation. To complete the model, we must determine Δ_1 and Δ_2. Since the ratio of the input white noise power to the (oscillator signal power)$\times\tau_1$ is small compared to both Γ_{12} and Γ_{21}, we may write

$$\Delta_1 = a\Gamma_{12} + \epsilon_1, \qquad \Delta_2 = a^{-1}\Gamma_{21} + \epsilon_2, \quad (14)$$

where a is a constant that we will determine shortly, and ϵ_1 and ϵ_2 are small compared to Γ_{12} and Γ_{21}. From Eq. (13), it follows that $P_1(\omega) \propto P_2(\omega) \propto 1/(\epsilon_1^2 + \omega^2\tau_1^2)$ with just white noise drivers when $\omega\tau_1 \ll 1$ and $\tau_2 \ll \tau_1$. We now find that

$$\begin{aligned} W_1 &= \frac{1}{4\epsilon_1\tau_1}\frac{\Delta_2^2 N_{1\mathrm{w}} + \Gamma_{12}^2 N_{2\mathrm{w}}}{\Delta_1\Delta_2 - \Gamma_{12}\Gamma_{21}}, \\ W_2 &= \frac{1}{4\epsilon_1\tau_1}\frac{\Delta_1^2 N_{2\mathrm{W}} + \Gamma_{21}^2 N_{1\mathrm{w}}}{\Delta_1\Delta_2 - \Gamma_{12}\Gamma_{21}}. \end{aligned} \quad (15)$$

Substituting Eq. (14) into (15), we find that $a = W_2/W_1$,

$$\epsilon_1 = \frac{N_{1\mathrm{w}}}{4\tau_1 W_1}\left(1 + \frac{W_2}{W_1}\frac{\Gamma_{12}^2}{\Gamma_{21}^2}\frac{N_{2\mathrm{w}}}{N_{1\mathrm{w}}}\right)^{-1}, \quad (16)$$

and $\epsilon_2 = (\Gamma_{12}/\Gamma_{21})(N_{2\mathrm{w}}/N_{1\mathrm{w}})\epsilon_1$.

Due to the dual injection locking, the quantities Δ_1 and Δ_2 are many orders of magnitude larger than Δ in the single-loop model. That has important implications for spur suppression. We note that both Γ_{21} and Γ_{12} must be non-zero for that to occur, from which we conclude that back-injection from the slave loop to the master loop is necessary.

As a final point, we have found in our experiments that the flicker noise in each loop depends on the loop length. A model for the flicker noise that we have found fits our data is

$$N_{1,2\mathrm{f}} = \left[10^{-12} + 10^{-11}(\tau_{1,2}/\tau_{\mathrm{f}})\right](W_{1,2\mathrm{s}}/f), \quad (17)$$

where f is the frequency. We attribute the length-dependent portion of the flicker noise to some combination of fluctuations of the fiber's effective length and optical scattering processes inside the fiber, whose relative importance has yet to be determined; we attribute the length-independent portion of the flicker noise to electrical processes in the photo-detector, amplifiers, and other electronic components. The amount of the length-independent flicker noise is consistent with previous measurements by others.

IV. Computational results and analytical limits

Typical experimental values, referred to the photo-detector, are: $W_1 = W_2 = -23$ dBm, $N_{1\mathrm{w}} = -166$ dBm/Hz, $N_{2\mathrm{w}} = -170$ dBm/Hz, $\tau_1 = 20\ \mu$s, $\tau_2 = 0.2\ \mu$s, $\Gamma_{12}^2 = -30$ dB, and $\Gamma_{21}^2 = -20$ dB. In this case, our model yields Fig. 2, which shows $\mathcal{L}(f)$ in dBc/Hz. Some points to note are: (1) There is a -100 dBc/Hz suppression of the first spur. (2) There is an additional -6 dBc/Hz suppression of the second spur. (3) There is a plateau in the slave loop's phase noise beyond 1 kHz. All these points can be explained by studying Eq. (13) in the appropriate asymptotic limits.

In considering simple asymptotic limits of Eq. (13), we will set $N_1(\omega) = N_2(\omega)$ and $W_1 = W_2$. We will also assume $\Gamma_{21}^2 \gg \Gamma_{12}^2$. These assumptions are not really necessary, but they help clarify the behavior. When we are close to resonance,

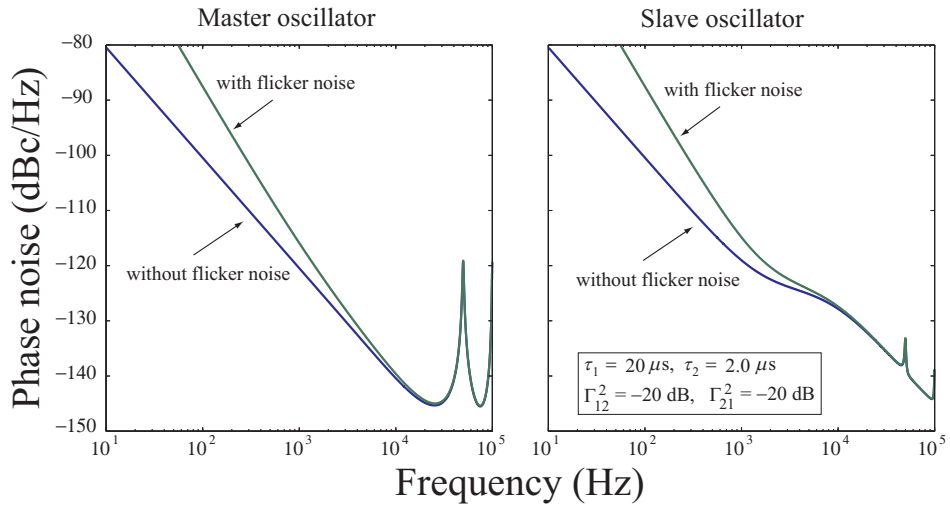

Fig. 3. Bode plots of the phase noise $\mathcal{L}(f)$ vs. frequency for both the master and slave loops. The parameters are modified from Fig. 2 in order to reduce the spurs.

we may write $|1-(1-\Delta_2)\exp(-j\omega\tau_2)|^2 \simeq \Delta_2^2 = \Gamma_{21}^2$ and $|1-(1-\Delta_1)\exp(-j\omega\tau_1)|^2 \simeq \Delta_1^2 + \omega\tau_1^2 = \Gamma_{12}^2 + \omega^2\tau_1^2$, so that

$$\frac{P_1(\omega)}{N_2(\omega)} = \frac{1}{\epsilon_1^2 + \omega^2\tau_1^2}, \qquad \frac{P_2}{N_1(\omega)} = \frac{1+\omega^2\tau_1^2/\Gamma_{21}^2}{\epsilon_1^2+\omega^2\tau_1^2}. \quad (18)$$

Hence, a plateau will appear in the slave loop's phase noise when $\omega\tau_1/\Gamma_{21} > 1$. For the parameters of Fig. 2, the point $\omega\tau_1/\Gamma_{21} = 1$ occurs when $f = \omega/2\pi = 796$ Hz. Physically, this frequency corresponds to the Leeson frequency, beyond which the phase of the slave loop is no longer locked to the phase of the master loop [15].

When we are close to a spur of the master loop, so that $\omega = 2\pi n/\tau_1$, where $n = 1, 2, \ldots$, then we find $|1-(1-\Delta_2)\exp(j\omega\tau_2)|^2 \simeq \Delta_2^2 + (2\pi n\tau_2/\tau_1)^2 = \Gamma_{21}^2 + (2\pi n\tau_2/\tau_1)^2$. We also find $|1-(1-\Delta_1)\exp(-j\omega\tau_1)|^2 \simeq \Delta_1^2 = \Gamma_{12}^2$, so that

$$\begin{aligned}\frac{P_1(\omega)}{N_1(\omega)} &= \frac{1+(2\pi n\tau_2/\Gamma_{21}\tau_1)^2}{\epsilon_1^2+(\Gamma_{12}/\Gamma_{21})^2(2\pi n\tau_2/\tau_1)^2},\\ \frac{P_2(\omega)}{N_2(\omega)} &= \frac{1}{\epsilon_1^2+(\Gamma_{12}/\Gamma_{21})^2(2\pi n\tau_2/\tau_1)^2}.\end{aligned} \quad (19)$$

When $n = 1$, this formula predicts a suppression of -97 dB for the first spur and an additional -6 dB suppression for the second spur, given the parameter set in Fig. 2. We note that the suppression is maximized by minimizing the master-to-slave coupling and increasing the time delay in the slave loop, as long as $2\pi\tau_2/\Gamma_{21}\tau_1 < 1$. For our parameters, we have $2\pi\tau_2/\Gamma_{21}\tau_1 = 0.628$, which is close to 1. We also find that the suppression of the spurs is maximized by maximizing the slave-to-master coupling. However, this coupling also increases the phase noise; so, there is a tradeoff between minimizing the phase noise and minimizing the spurs.

We can use Eq. (13) to suggest regimes in which it is possible to obtain significantly greater suppression of the spurs without greatly increasing the phase noise. In particular, Eq. (13) suggests that we would do better by equalizing the master-to-slave and slave-to-master coupling and by increasing the length of the slave loop. In Fig. 3, we show $\mathcal{L}(f)$ where we increase τ_2 to 2 μs and increase Γ_{12}^2 to -20 dB, without changing the other parameters in Fig. 2. We see that there is almost -120 dB suppression of the first spur in the master loop and more than -130 dB suppression in the slave loop, with very little phase noise penalty. With these parameters, it remains to theoretically examine the behavior in the neighborhood of 500 kHz and determine experimentally whether in practice the noise drivers remain the same. However, these results certainly make clear that there is a large amount of room for improvement.

V. Conclusions

We have presented an extension of the Yao-Maleki model to two coupled oscillators, and we have applied this model to the DIL-OEO configuration. This model appears to be in good agreement with experiments and full simulations, to within about 5 dB, although a careful comparison must still be carried out. The model complements a full simulation model that we have developed that is dynamical and keeps all the nonlinear effects, so that the full model can determine the locking bandwidth and stability, in addition to the phase noise spectrum during steady-state operation. The simple model presented here will allow us to rapidly scan the parameter space in order to optimize the performance of the DIL-OEO. While there are difficult tradeoffs between close-in phase noise and spurs, our results to date suggest that significant improvements over our current experimental configuration are possible.

References

[1] R. C. Williamson and R. D. Esman, "RF photonics," *J. Lightwave Technol.*, vol. 26, no. 9, pp. 1145–1153, May 2008.

[2] X. S. Yao and L. Maleki, "Converting light into spectrally pure microwave oscillation," *Opt. Lett.*, vol. 21, no. 7, Apr. 1996.

[3] X. S. Yao and L. Maleki, "Optoelectronic microwave oscillator," *J. Opt. Soc. Am. B*, vol. 13, no. 8, pp. 1725–1735, Aug. 1996.

[4] D. A. Howe and A. Hati, "Low-noise X-band oscillator and amplifier technologies: Comparison and status," *Proc. 2005 Joint Meeting IEEE International Frequency Control Symposium and Precise Time and Time Interval Systems and Applications*, pp. 481–487, Aug. 2005.

[5] X. S. Yao and L. Maleki, "Multiloop optoelectronic oscillator," *IEEE J. Quantum Electron.*, vol. 36, no. 1, Jan. 2000.

[6] W. Zhou and G. Blasche, "Injection-locked dual opto-electronic oscillator with ultra-low phase noise and ultra-low spurious level," *IEEE Trans. Microwave Theory Tech.*, vol. 53, no. 3, Mar. 2005.

[7] N. Yu, E. Salik, and L. Maleki, "Ultralow-noise mode-locked laser with coupled optoelectronic oscillator configuration," *Opt. Lett.*, vol. 30, no. 10, May 2005.

[8] O. Okusaga, W. Zhou, G. M. Carter, and C. R. Menyuk, "Investigating the forward and backward injections of injection-locked dual optoelectronic oscillators," *Proc. 2009 Optical Fiber Communications Conf.*, San Jose, CA, Mar. 24–26, 2009.

[9] E. C. Levy, M. Horowitz, and C. R. Menyuk, "Noise distribution in the radio frequency spectrum of optoelectronic oscillators," *Opt. Lett.*, vol. 33, no. 24, pp. 2883–2885, Dec. 2008.

[10] E. C. Levy, M. Horowitz, and C. R. Menyuk, "Modeling optoelectronic oscillators," *J. Opt. Soc. Am. B*, vol. 26, no. 1, pp. 148–159, Jan. 2009.

[11] E. C. Levy, M. Horowitz, C. R. Menyuk, O. Okusaga, W Zhou, and G. M. Carter, "Study of dual-loop optoelectronic oscillators," *Proc. Joint Meeting IEEE Frequency Control Symposium and the European Frequency and Time Forum*, Besançon, France, Apr. 21–24, 2009.

[12] O. Okusaga, W. Zhou, E. C. Levy, M. Horowitz, G. M. Carter, and C. R. Menyuk, "Experimental and simulation study of dual injection-locked OEOs," *Proc. 2009 Joint Meeting IEEE Frequency Control Symposium and the European Frequency and Time Forum*, Besançon, France, Apr. 21–24, 2009.

[13] E. C. Levy, M. Horowitz, C. R. Menyuk, O. Okusaga, W. Zhou, and G. M. Carter, "Modeling opto-electronic oscillators," *Proc. 2009 Conf. Lasers and Electro-Optics and Int. Quantum Elctronics Conf.*, Baltimore, MD, Jun. 1–5, 2009.

[14] O. Okusaga, W. Zhou, E. C. Levy, M. Horowitz, G. M. Carter, and C. R. Menyuk, "Non-ideal loop-length-dependence of phase noise in OEOs," *Proc. 2009 Conf. Lasers and Electro-Optics and Int. Quantum Elctronics Conf.*, Baltimore, MD, Jun. 1–5, 2009.

[15] E. Rubiola, *Phase Noise and Frequency Stability in Oscillators*, Cambridge U. Press, 2009.